Ultrafast plasmonic field oscillations and optics of molecular resonances caused by coherent exciton-plasmon coupling

S. M. Sadeghi*

Department of Physics, University of Alabama in Huntsville, Huntsville, Alabama 35899, USA and
Nano and Micro Device Center, University of Alabama in Huntsville, Huntsville, Alabama 35899, USA

(Received 18 February 2013; revised manuscript received 21 May 2013; published 22 July 2013)

We study optical properties and coherent dynamics of a hybrid system consisting of one quantum dot and one metallic nanoparticle when its excitations are governed by its collective molecular states (dark and bright states), rather than excitons or plasmons. We predict that in the bright state the exciton states of the quantum dot are optically dressed, forming standard Mollow spectra with ac Stark shifts enhanced by plasmonic effects. In the dark state the optics of the quantum dot is dominated by a combination of two seemingly uncorrelated processes: (i) coherent generation of a superfluorescent state that supports ultranarrow gain in the absence of population inversion, and (ii) plasmonic broadening and red shifting of pure exciton states, as if the laser field does not exist. We show that the coherent exciton-plasmon coupling in such a system can form an analog of Rabi flopping in the plasmonic field, causing its ultrafast oscillation, when the laser is red detuned from the quantum dot transition. For blue-detuning we predict generation of time delay in the field experienced by the quantum dot, before the system is transferred to its dark state.

DOI: 10.1103/PhysRevA.88.013831 PACS number(s): 42.50.Nn, 78.67.Hc, 42.65.Pc, 71.35.Cc

I. INTRODUCTION

Recent studies have shown that quantum coherence in systems consisting of one semiconductor quantum dot (QD) and a metallic nanoparticle (MNP) can drastically change their physical and optical properties, offering novel applications and concepts. For example, these effects allow us to induce Rabi frequency [1–3], control speed of light [4], and generate bistability and hysteresis [5–7]. Recent studies have also shown that quantum coherence in QD-MNP systems can be used to change energy dissipation rates in the MNPs [5,8–13], reverse the course of energy transfer, allowing flow of energy from the MNPs to the QDs [14], and to generate plasmonically induced transparency and slow light in multilevel QD systems [15].

One of the essential features of a QD-MNP system is the fact that, because of exciton-plasmon coupling induced by quantum coherence, the QD normalizes the plasmonic field that it experiences. This allows this system to exhibit collective molecularlike states and resonances, different from excitons or plasmons [16]. Figure 1 schematically shows the differences between the optical excitations in an isolated QD (a) and in a QD-MNP system supporting such collective states (b). $|1\rangle$ and $|2\rangle$ in (a) refer, respectively, to the ground and fundamental exciton states of the QD. In the case of the QD-MNP system, however, we are dealing with two collective states, $|D\rangle$ (dark state) and $|B\rangle$ (bright state). For a given frequency of the laser field (ω_l), the system can be excited to either the B or D state, depending on the intensity of the laser. Therefore, these states can be doubly degenerate, although they may have different energy dissipation rates [17]. By changing the intensity of the laser field around a critical value (I_c) one can switch the state of QD-MNP molecule between B and D states, although their transition energies or laser frequency remains unchanged.

Our objective in this paper is to investigate quantum optical properties and coherent dynamics of QD-MNP systems when their excitations are governed by their collective molecular resonances (or B and D states), rather than the pure exciton or plasmon resonances. For this we use linear absorption and resonance fluorescence (RF) spectra of the QDs to demonstrate dramatic differences in the nature of the interaction between light and these systems when they are excited to the B or D state [Fig. 1(b)]. We show that in the B state the QD can emit efficiently and its exciton states are dressed by the laser field, similar to the case of an isolated QD. Under this condition the QD supports standard Mollow spectra [18,19], while the combined effects of plasmons and quantum coherence lead to enhancement of their ac Stark shifts. In contrast to the common understanding [20], however, although here the QD and MNP are close to each other, in this state, we do not predict any significant linewidth broadening or transition red shift via plasmonic effects. In other words, the impact of plasmonic effects is mainly field enhancement, and induction of energy transfer from the QD to the MNP is suppressed.

When the QD-MNP system is excited to the D state, however, the nature of its interaction with the laser field changes significantly. In this state the QD does not emit efficiently, rather the energy of the QD-MNP system mostly serves to warm up the MNP [17]. Under these conditions, the optical properties of the QD are mostly determined by combination of two components: (i) coherent formation of an ultranarrow superfluorescent state which supports gain in the absence of population inversion, and (ii) the pure exciton states of the QD as if the laser field does not exist. In the latter the QD transition is strongly broadened and red shifted, similar to the case when the quantum coherence effects do not exist. These results support nearly instantaneous transition between high to zero resonance fluorescence states and between transparency to high gain states of the QD-MNP systems.

In this paper we also investigate the impact of coherent exciton-plasmon coupling in the dynamic of the QD-MNP

*seyed.sadeghi@uah.edu

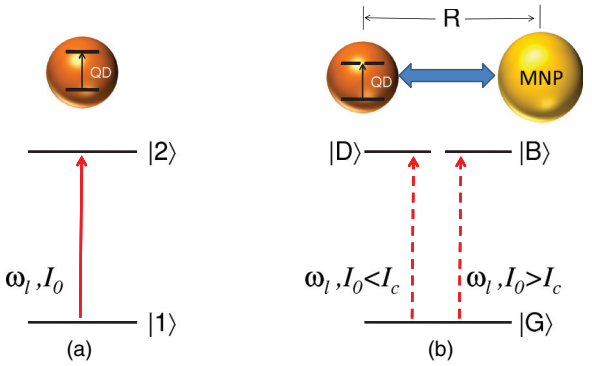

FIG. 1. (Color online) Schematic illustrations of the electronic structures of an isolated QD (a) and that of a QD-MNP system in the presence of quantum coherence. $|1\rangle$ and $|2\rangle$ refer, respectively, to the ground and fundamental exciton states of the QD. $|B\rangle$ and $|D\rangle$ represent the collective metastates (B and D states) of the QD-MNP system.

system when the laser field is tuned around the QD resonance. For red detuning, i.e., when the laser frequency is smaller than that of the exciton, our results suggest formation of an analog of Rabi floppy in the coherently normalized plasmonic field of the MNP, causing its ultrafast oscillations. Under these conditions, the absorption spectrum of the QD forms ultradispersive features, suggesting strong enhancement of the competition between gain and absorption processes. On the other hand, for blue detuning, i.e., the case when the laser frequency is larger than that of the exciton, we predict fundamentally different dynamics. Here, compared to the applied field, with the increase of the detuning the effective field experienced by the QD is exceedingly delayed. When such a detuning reaches a specific limit the time delay becomes infinite, suppressing $P_{\rm coh}$ at all times as the system is transferred into its D state.

II. COHERENT INTERACTION OF LIGHT WITH QUANTUM DOT-METALLIC NANOPARTICLE SYSTEMS

The system considered in this paper consists of a spherical Au MNP with a radius (a) and a QD, separated from each other with the center-to-center distance R. The upper state of the QD ($|2\rangle$) can decay via Forster resonance energy transfer (FRET) to the MNP or its intrinsic radiative and nonradiative transitions. We consider the environment holding this system has the dielectric constant ε_0. This system interacts with a laser field $E = E_0\cos(\omega_l t)$ near resonant with the $|1\rangle$-$|2\rangle$ (1-2) transition with ω_{12} frequency. The interaction between the QD and the MNP is characterized by the large electric dipole moments of the QD and plasmon resonance of the MNP. The dimension of the MNP is considered small enough to ignore higher multipole contributions [21]. The dielectric function of the MNP ($\varepsilon_m(\omega)$) includes contributions of both d electrons (ε^d) and the Drude contributions (ε^s) given by

$$\varepsilon^s(\omega) = 1 - \frac{\omega_p^2}{\omega[\omega - i\Gamma(a)]}. \tag{1}$$

Here $\Gamma(a) = \Gamma_\infty + \frac{Av_F}{a}$ is the electron scattering rate of the MNP. Γ_∞ is the bulklike electron scattering rate considered equal to 0.1 eV [22], and $v_F = 1.4\times10^8$ cm/s is the Fermi velocity. A is a model-dependent constant taken to be equal to one [22]. ω_p refers to the plasmon frequency of Au. The values of ε^d for Au at different frequencies were taken from Ref. [22].

Considering these and the master equation,

$$\dot\rho = -\frac{i}{\hbar}[H_{QD},\rho] + \dot\rho|_{\rm relax}, \tag{2}$$

where $\dot\rho|_{\rm relax}$ refers to the relaxation terms that do not depend on plasmonic effects, we obtained the elements of the density matrix (ρ_{ij}). Under the steady-state condition (ss) these elements are as follows [3]:

$$\rho_{22}^{ss} = \frac{2{\rm Im}\left[\Omega_{12}^0\left(1+\frac{2\gamma a^3}{R^3}\right)\rho_{21}^{ss}\right] - 2\Gamma_F\left|\rho_{21}^{ss}\right|^2}{\Gamma_{22}}, \tag{3}$$

and

$$\rho_{21}^{ss} = -\frac{i\Omega_{12}^0\left(1+\frac{2\gamma a^3}{R^3}\right)\left(\rho_{11}^{ss}-\rho_{22}^{ss}\right)}{[-i\Delta_{\rm eff}+\Lambda_{\rm eff}]}. \tag{4}$$

Here $\gamma = \frac{\varepsilon_m(\omega_l)-\varepsilon_0}{\varepsilon_m(\omega_l)+2\varepsilon_0}$, $\Omega_{12}^0 = -\frac{\mu_{12}E_0}{2\hbar\varepsilon_{\rm eff1}}$ is the Rabi frequency, and $\Gamma_F = {\rm Im}[\eta]$ refers to the Forster energy transfer from $|2\rangle$ to the MNP ($\eta = \frac{4\gamma\mu_{12}^2}{\hbar\varepsilon_{\rm eff1}^2}\frac{a^3}{R^6}$). $\Delta_{\rm eff}$ is the effective detuning of the QD from the laser field given by

$$\Delta_{\rm eff} = \Delta_{12} + {\rm Re}[\eta]\left(\rho_{11}^{ss}-\rho_{22}^{ss}\right), \tag{5}$$

where $\Delta_{12} = \hbar(\omega_l - \omega_{12})$. On the other hand $\Lambda_{\rm eff}$ represents the effective damping of ρ_{12}^{ee}. It is given by

$$\Lambda_{\rm eff}(\omega_l, I_l) = \gamma_{21} + \Gamma_F\left(\rho_{11}^{ss}-\rho_{22}^{ss}\right), \tag{6}$$

wherein γ_{21} corresponds to broadening of the 1-2 transition in the absence of the MNP. In Eqs. (5) and (6) we explicitly show the dependence of $\Lambda_{\rm eff}$ and $\Delta_{\rm eff}$ on the laser intensity (I_0) and frequency. Considering Eq. (4) we can also calculate the plasmonic field enhancement including quantum coherence as follows [2,3]:

$$P_{\rm coh} = \left|1 + \frac{2\gamma a^3}{R^3} + \frac{\eta}{\Omega_{12}^0}\rho_{21}^{ss}\right|^2. \tag{7}$$

Note that $\Gamma_F|\rho_{21}^{ss}|^2$ in Eq. (3) refers to the FRET-induced energy relaxation of excitons. Additionally, $\Omega_{12}^0(1+\frac{2\gamma a^3}{R^3}) \equiv \Omega_{\rm eff}$ represents the way plasmonic effects (in the absence of quantum coherence) influences the Rabi frequency of the QD. Γ_{22} refers to the radiative decay rate of excitons in the QD. For ρ_{11} we used the fact that $\dot\rho_{11} = -\dot\rho_{22}$.

The linear absorption of the QD $A(\omega_p)$ was found using

$$A(\omega_p) \propto {\rm Re}\int_0^\infty \langle[P^-(t'+\tau), P^+(t')]\rangle e^{i\omega_p\tau}d\tau, \tag{8}$$

where P^+ and P^- are, respectively, the positive and negative frequency components of the system polarization. $\tau = t - t'$ where the time $t > t'$ [18]. Under steady-state conditions ($t,t' \to \infty$) $A(\omega_p)$ is obtained as [10]

$$A(\omega_p) = {\rm Re}\Big[\mu_{12}^2\big\{\rho_{21}^{ss}[R_{32}(z) - R_{31}(z)] - R_{33}(z)\left[\rho_{11}^{ss}-\rho_{22}^{ss}\right]\big\}\Big]_{z=i\omega_p}, \tag{9}$$

where ω_p refers to the frequency of the probe field. Here R_{nm} are the elements of $\mathbf{R}(z) = (z\mathbf{I}-\mathbf{L})^{-1}$, wherein $\mathbf{I}$ is a

4×4 identity matrix and $\mathbf{L}$ is the coefficient of ρ_{ij} obtained from Eq. (2). On the other hand RF ($S(\omega_p)$) was obtained from [18,23]

$$S(\omega_p) = \mathrm{Re}\int_0^\infty \langle P^-(t'+\tau)P^+(t')\rangle e^{i\omega_p\tau}d\tau. \qquad (10)$$

Under steady state we found the following expression for S:

$$S(\omega) = \mu_{12}^2 \mathrm{Re}\left[R_{3,1}(z)\rho_{21}^{ee} + R_{3,3}(z)\rho_{22}^{ee}\right]_{z=i\omega_p}. \qquad (11)$$

III. DOUBLY DEGENERATE COLLECTIVE STATES OF QD-MNP SYSTEMS

We start with the review of B and D states in the QD-MNP system described in the preceding section. For this we consider the MNP is made of Au and its radius (a) is 7 nm. We also consider the dielectric constant of the environment (ε_0) is 1.8, allowing the MNP to have plasmonic at about 2.3 eV. Moreover in this paper we assume $\Gamma_{22} = 1/1.7\,\mathrm{ns}^{-1}$, $\mu_{12} = 0.65\,e \times \mathrm{nm}$, $\gamma_{21} = 3.3\ \mathrm{ns}^{-1}$ [5,9,16].

Figure 2 shows variations of P_{coh} as a function of R when $\Delta_{12} = 0$ and the intensity of the laser (I_0) is 217.9 (circles), 13.6 (squares), and 0.5 W/cm^2 (triangles). The results suggest that for both cases with the reduction of R, P_{coh} increases, as one expects. This trend continues until we reach a critical distance (R_c) where P_{coh} decreases abruptly. This distance is smaller for larger I_0. These results suggest that the QD-MNP system supports two collective states. For a given laser intensity, when $R > R_c$ the system is in the B state, i.e., the QD emits efficiently. When $R < R_c$ and P_{coh} becomes very small and, therefore, the QD emission efficiency is reduced. More specifically, considering the results shown in Fig. 2, if $R < 16.4$ nm, interaction of the QD-MNP system with a laser field with the intensity 13.6 W/cm^2 causes excitation to the D state. When $R > 16.4$ nm the system is excited to the B state. A similar argument can be made for the case when $I_0 = 217.9$ W/cm^2. As shown in Fig. 2 (triangles), when the laser intensity is quite low the abrupt change in P_{coh} is smeared out but its suppression starts at a larger value of R.

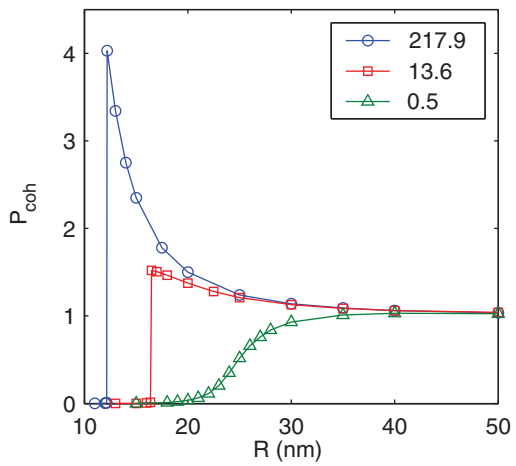

FIG. 2. (Color online) Variation of P_{coh} as a function of R when the laser intensity (I_0) is 217.9 (circles), 13.6 (squares), and 0.5 W/cm^2 (triangles).

The interpretation of the results shown in Fig. 2 in terms of optical excitation of the QD-MNP system via its collective resonances [Fig. 1(b)] becomes clearer considering the fact that for a reasonably small R we can adjust I_0 to selectively excite the system to the B or D state. Note that this system supports a critical value for I_0 (I_c) such that when $I_0 > I_c$ the system is excited to the B state and when $I_0 < I_c$ it ends up with the D state. For example, when $R = 16.4$ nm and $I_0 < 13.6$ W/cm^2 the QD-MNP system is excited to the D state. When $I_0 > 13.6$ W/cm^2, the B state is its final state. In other words, here $I_c = 13.6$ W/cm^2. Since this process happens without changing the frequency of the laser field, we may conclude that under these conditions, the B and D states are degenerate, as schematically shown in Fig. 1(b). They can, however, be excited selectively by adjusting the intensity of the laser when its frequency is kept unchanged.

IV. QUANTUM OPTICAL PROPERTIES OF THE QD IN DARK AND BRIGHT STATES

To investigate the optical properties of the QD when its excitation is determined by the collective states of the QD-MNP system, rather than by pure plasmons and excitons, in Fig. 3 we study the linear absorption (a) and RF (b) spectra of the QD. For this we consider $R = 100$ (solid line) and 17 nm (dashed line) as a function of $\Delta_p = \omega_p - \omega_{12}$ when $I_0 = 13.6$ W/cm^2. The solid line refers to the case when the effects of plasmons are ignorable (nearly isolated QD), and the dashed line to the case of when the system is in the B state. The results suggest that in this state, compared to that of an isolated QD, the plasmonic effects act as if the laser field intensity is increased. The spectra seen in Fig. 3(a) are

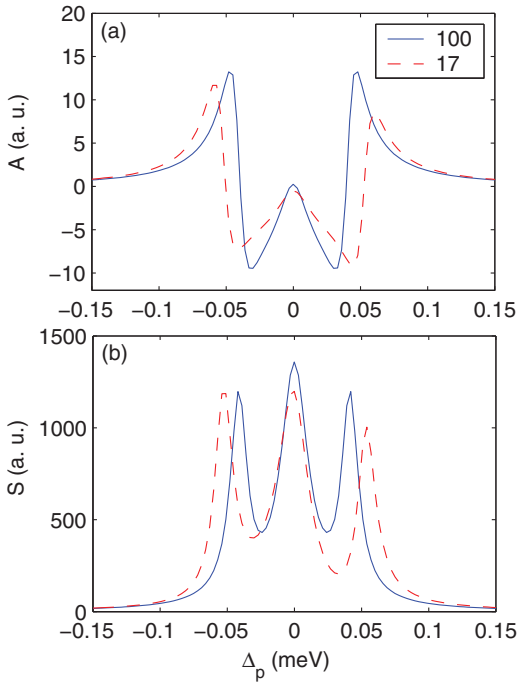

FIG. 3. (Color online) Absorption (a) and RF (b) of the QD for different values of R (legends in nm) when the laser intensity is 13.6 W/cm^2. Here the QD-MNP is the B state. $\Delta_p = \hbar(\omega_p - \omega_{12})$ is the tuning of the probe field with frequency ω_p from the QD transition.

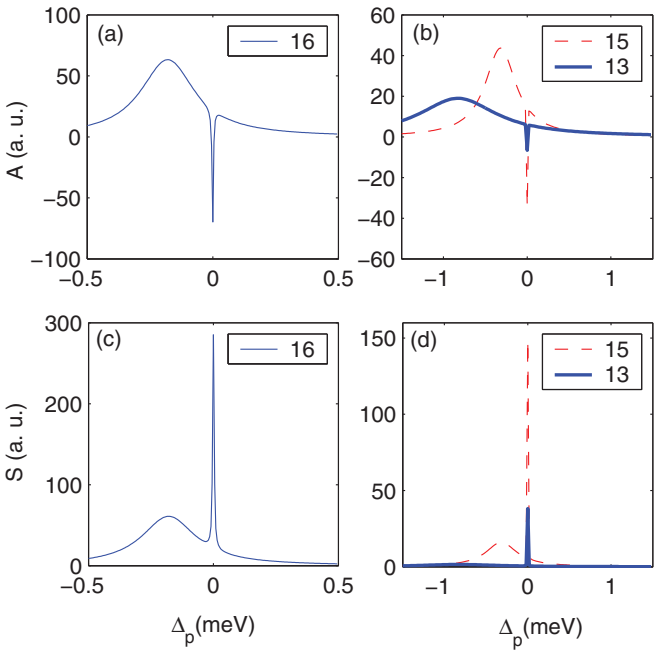

FIG. 4. (Color online) Absorption [(a), (b)] and RF [(c), (d)] of the QD for different values of R (legends in nm). Here the QD-MNP system in the D state. All other specifications are the same as those in Fig. 3.

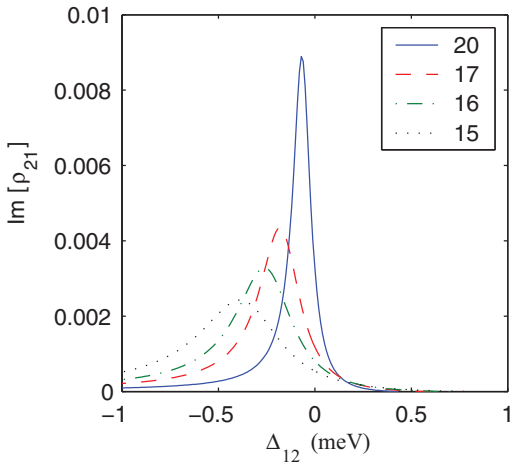

FIG. 5. (Color online) Imaginary part of ρ_{12} for different values of R (legends in nm) when the laser intensity is 13 mW/cm^2. All other specifications are the same as those in Fig. 3.

in fact Mollow spectra [18], which are modified by the near field of the MNP plasmons. Therefore, in the B state the optics of the QD follows the dressed state picture with modified energy separation, as discussed in the following in detail. This is obvious considering the results shown in Fig. 3(b), wherein we see the triplet RF Mollow spectra with frequency shifts enhanced by plasmonic effects (dashed line). Experimental observation of Mollow spectra of isolated QDs has recently been reported [19].

The results shown in Fig. 4(a) suggest that when R reaches 16 nm, and the system is transferred to the D state (Fig. 2, squares), the response of the QD changes dramatically. Here the absorption spectrum consists of an ultranarrow gain feature at the laser wavelength and a broad red-shifted absorption peak. As shown in Fig. 4(b), with further reduction of R the frequency of the narrow gain peak remains unchanged but that of the broad peak is red shifted further while becoming more broadened. These results also show that with the reduction of R the amplitudes of both the broadened peak and ultranarrow features are reduced, indicating reduction of the exciton population.

The results shown in Figs. 4(c) and 4(d) indicate significant changes in the RF spectra of the QD. These results suggest that with reduction of R from 17 to 16 nm, the triplet Mollow spectra are replaced with two distinct seemingly unrelated features, i.e., a broadened peak and an ultranarrow superfluorescent line. As shown in Fig. 4(d) (solid line), when $R = 13$ nm the contribution of the broadened peak vanishes but the ultranarrow resonance fluorescence remains quite evident. Note that the overall efficiency of the QD in the cases of Figs. 4(c) and 4(d) (D state) is much smaller than that in Fig. 3(b) (B state).

Inspection of the results shown in Fig. 4 suggests that in the D state we are basically dealing with two different types of optical processes, one that leads to the broadened red-shifted peak and the other that causes the ultranarrow feature. The former has features very similar to the case when we consider plasmonic effects of an MNP in the absence of quantum coherence or when the laser field intensity is very weak. To see this in Fig. 5, we study variations of Im[ρ_{12}] corresponding to absorption of the QD in the limit when $I_0 = 13$ mW/cm^2 for different R (legends in nm). The results show large similarities with the broad peak spectra seen in Figs. 4(a) and 4(b). Considering this we believe the broad spectra in Fig. 4 are associated with decoupling of the QD-MNP system from the laser field. The impact of this field, however, is translated into generation of the ultranarrow peak. This peak is not the result of coherent scattering, as Eq. (11) does not include such a process. The nature of the gain can be traced back to the fact that under no circumstance we expect to see population inversion in the two-level QD system. Gain with inversion can happen in its dressed states. In fact this is the reason of seeing gain in the case of the B state. In the case of the D state, however, the system does not support the dressed state. We believe the ultranarrow gain in the D state is caused by coherent transfer of energy from the laser field into a coherently induced state with a wavelength the same as that of the laser field, causing gain without inversion [24].

V. RESONANCE ASYMMETRY VIA EXCITON-PLASMON COUPLING

For the results shown in Fig. 4 we considered the laser field is resonance with the 1-2 transition, i.e., $\Delta_{12} = 0$. These results suggest that in the B state the broad peak occurs in the red side of this transition. As mentioned in the preceding section, this peak is caused by the pure plasmonic effects in the absence of quantum coherence (Fig. 5). To gain a clearer picture of the coherent molecular resonance in the QD-MNP system and the impact of exciton-plasmon coupling in the QD transition, in this section we study the absorption spectra of the QD while

tuning the laser frequency around the 1-2 transition for both $\omega_l > \omega_0$ ($\Delta_{12} > 0$) and $\omega_l < \omega_0$ ($\Delta_{12} < 0$). As shown in the following, the latter allows that as the laser frequency reaches the broad peak, exciton-plasmon coupling leads to ultrafast oscillations of the plasmonic field enhancement factor ($P_{\rm coh}$) and enhances gain or absorption dispersive features. For the case of $\Delta_{12} > 0$ we demonstrate switching between the D and B states.

We start with the case of $\Delta_{12} > 0$ when $R = 14$ nm and $I_0 = 78.4$ W/cm^2 and other specifications are the same as those in Fig. 3. The results shown in Fig. 6 show that when $\Delta_{12} = 0.03$ meV the spectrum becomes asymmetric, becoming similar to the standard Mollow spectrum under detuned coupling of the 1-2 transition (dashed line) [25]. As shown in Fig. 6(b), the situation changes abruptly when Δ_{12} becomes 0.05 meV. Under this condition, the system is transferred to its D state and its spectrum becomes similar to those in Fig. 4. As shown in Fig. 6(c), further increase of Δ_{12} leads to more blue shift of the ultranarrow gain feature while it is suppressed in amplitude.

The results shown in Fig. 7 suggest that for $\Delta_{12} < 0$ the absorption spectrum of the QD changes quite differently. These results suggest that with the increase of $|\Delta_{12}|$ under this condition the dispersive feature of the Mollow spectrum, which happens at the laser frequency, evolves in a peculiar way. This feature is shown to be the result of interference between gain and absorption processes [25]. Our results in Fig. 7 suggest that when the laser frequency reaches that of the broad

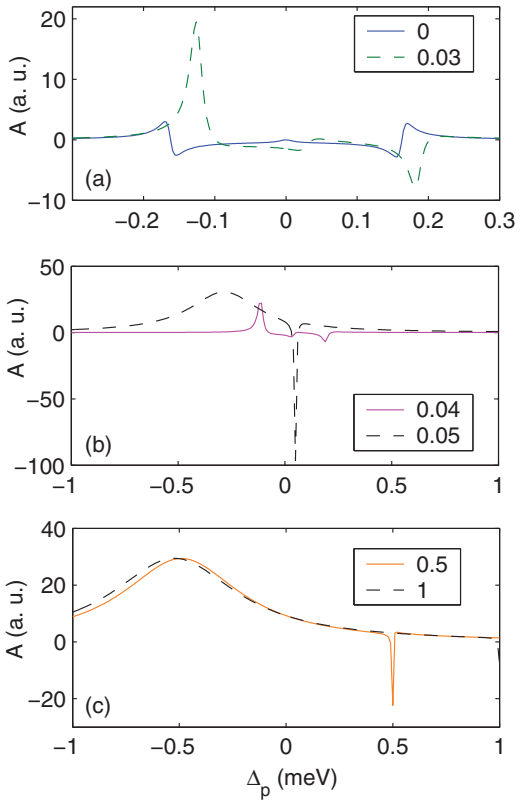

FIG. 6. (Color online) Absorption of the QD for different values of detuning of the laser field from the 1-2 transition (Δ_{12}) when $\omega_l > \omega_{12}$ (legends in meV). Here $R = 14$ nm and $I_0 = 78.6$ W/cm^2. All other specifications are the same as those in Fig. 3.

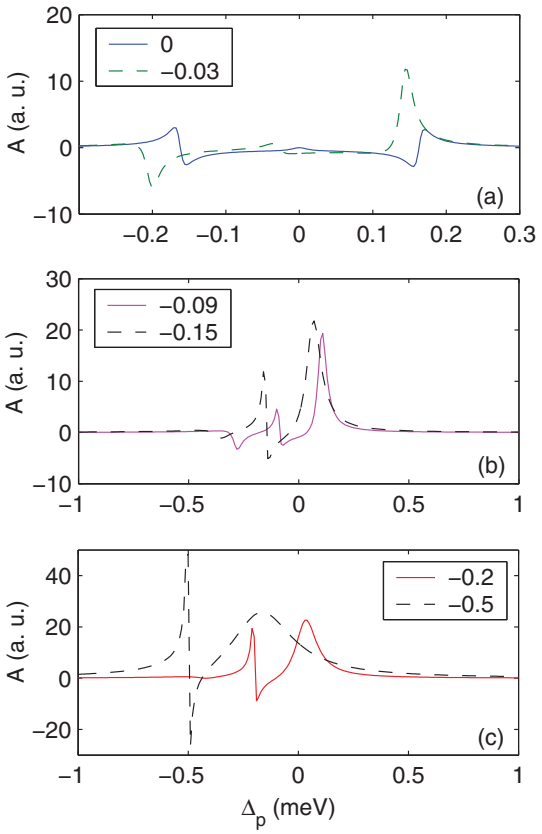

FIG. 7. (Color online) Absorption of the QD for different values of detuning of the laser field from the 1-2 transition (Δ_{12}) when $\omega_l < \omega_{12}$ (legends in meV). Here $R = 14$ nm and $I_0 = 87.6$ W/cm^2. All other specifications are the same as those in Fig. 3.

peak, the system stays in the B state but the linear absorption spectrum evolves into Mollow spectra with enhanced gain or absorption dispersive features [Fig. 7(b)]. With further increase of $|\Delta_{12}|$ the broad peak starts to resume its spectral feature, while the dispersive features become significantly pronounced [Fig. 7(c), dashed line]. This may suggest that coherent exciton-plasmon coupling in QD-MNP can enhance the interference between the gain and absorption at the laser frequency, increasing their amplitudes and dispersion.

To obtain further insight in the governing physics behind the results shown in Figs. 6 and 7, in Fig. 8 we study variation of $P_{\rm coh}$ for the two cases of positive and negative Δ_{12}. The results show that with the decrease of the laser frequency ($\Delta_{12} < 0$) $P_{\rm coh}$ starts to increase, reaching the value of 7.2 at $\Delta_{12} \sim -0.5$ meV (squares). As $|\Delta_{12}|$ increases beyond this value, $P_{\rm coh}$ decreases, approaching the intrinsic value of plasmonic field enhancement in the absence of quantum coherence (dashed line).

The situation is rather different for $\Delta_{12} > 0$. Here before Δ_{12} reaches 0.05 meV, $P_{\rm coh}$ decreases continuously. When Δ_{12} becomes equal to 0.05 meV, however, its value is abruptly suppressed. This process, which is shown clearly in the inset of Fig. 8, corresponds to the transition from the B to D state, as also seen in Fig. 6(b). As Δ_{12} increases further $P_{\rm coh}$ starts to recover, reaching the intrinsic plasmonic field enhancement of

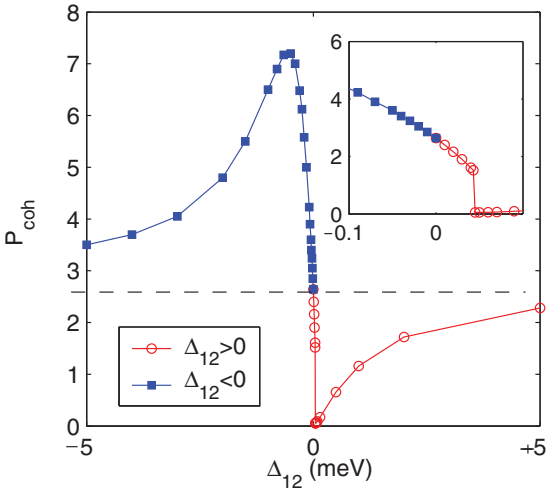

FIG. 8. (Color online) Variation of P_{coh} as a function of Δ_{12}. The horizontal dashed line refers to the intrinsic plasmonic field enhancement of the MNP at $R = 14$ nm in the absence of quantum coherence. All other specifications as those in Fig. 6.

the MNP in the absence of quantum coherence (dashed line). This is because of the fact that with large detuning the QD starts to decouple from the laser field.

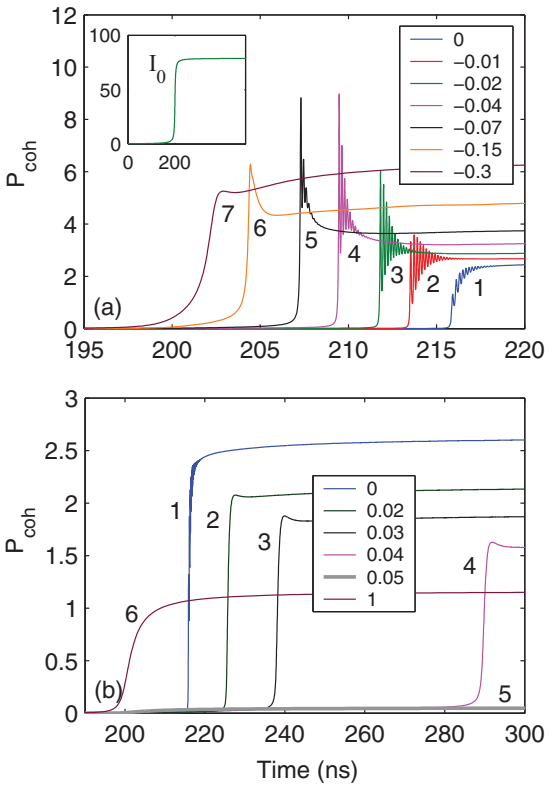

FIG. 9. (Color online) Variation of P_{coh} as function of time for different negative (a) and positive (b) values of Δ_{12} (legends in meV). Here the laser field has a rise time at 200 ns of the scale (inset) and its final intensity (I_0) is 78.4 W/cm^2. All other specifications are the same as those in Fig. 6.

VI. ULTRAFAST COHERENT OSCILLATION OF PLASMONIC FIELD

An interesting feature of the QD-MNP system studied in this paper happens when we study how Δ_{12} influences the way this system interacts with a time-dependent laser field. For this reason, in this section we consider the response of this system to the laser field at the very early time when it was turned on. In other words, as shown in the Fig. 9(a) inset, we assume the amplitude of this field increases from zero to a certain value corresponding to the final intensity (I_0) of 78.4 W/cm^2 at 200 ns of the scale. The results represented in the previous sections were obtained considering the response of the system at times well after this rise time.

The results reported in Fig. 9(a) (and in Fig. 10 with details) show dramatic upheaval of P_{coh} when $\Delta_{12} < 0$. These results show that for $\Delta_{12} = 0$ the rise time of P_{coh} happens at about

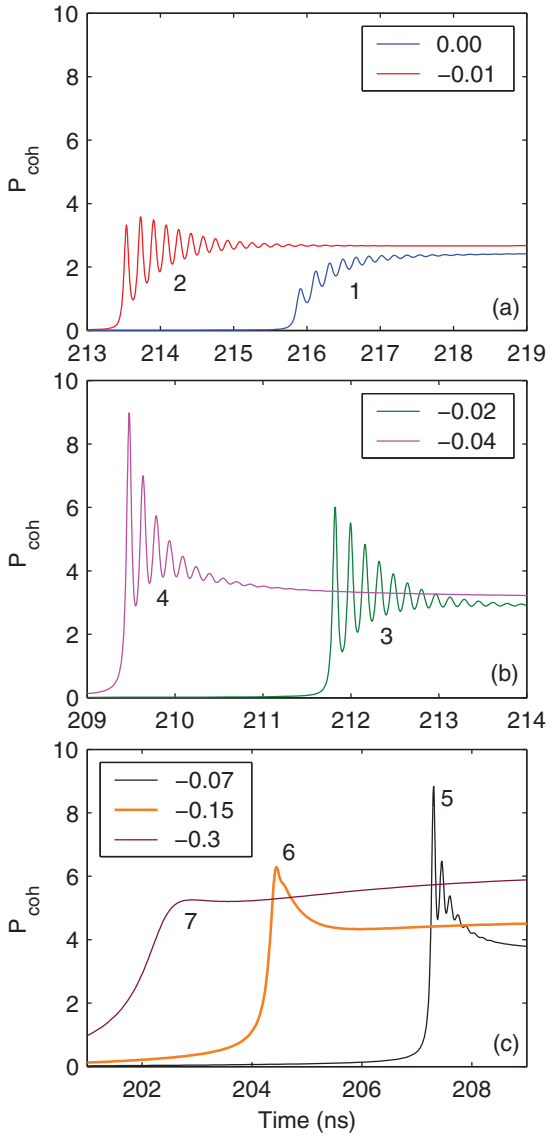

FIG. 10. (Color online) The same as Fig. 9(a). In (a) $\Delta_{12} = 0$ (line 1) and -0.01 meV (line 2), in (b) $\Delta_{12} = -0.02$ (line 3) and -0.04 meV (line 4), and in (c) $\Delta_{12} = -0.07$ (line 5), -0.15 meV (line 6), and -0.3 meV (line 7).

216 ns, indicating a slight delay compared to the rise time of the applied field. This process happens as P_{coh} initially undergoes low-amplitude oscillation, before it settles to its steady-state value [Fig. 9(a), line 1]. With the increase of $|\Delta_{12}|$ the rise time of P_{coh} starts to shift back to that of the applied field [Fig. 9(a), inset]. This occurs while the oscillation amplitudes and values of P_{coh} are increased. Figure 9(a) shows that for $\Delta_{12} \sim -0.04$ meV (line 4) the peak of P_{coh} reaches about 9. As $|\Delta_{12}|$ increases further the oscillation damping increases. $\Delta_{12} = -0.15$ meV, the system seems to be critically damped (line 6). For relatively large $|\Delta_{12}|$ (line 7), the value of P_{coh} declines and its rise time reaches 200 ns, as that of the applied field.

Figure 10 shows in more detail how the coherently induced oscillations of P_{coh} are evolved with Δ_{12}. For $\Delta_{12} = 0$ the period of the oscillations is about 190 ps while for $\Delta_{12} = -0.07$ meV, it reduces to about 150 ps. This is rather similar to Rabi flopping in atoms, wherein detuning of the laser increases its oscillation frequency [26]. The ultrafast oscillations of P_{coh} or effective field of the QD is an indication of coherent dynamics of the QD-MNP system when the laser field is tuned about the broad peak. In fact, as shown in Fig. 6, when $\Delta_{12} = 0$ the system is in the B state. As the laser field is detuned negatively, the effective field of the QD increases, since P_{coh} enhances (Fig. 8). On the other hand, as shown in Ref. [3], because of coherent-plasmon coupling the rise time of the effective field experienced by the QD, defined as $I_{eff} = I_0 P_{coh}$, can be much steeper than the rise of the applied field. To see this in Fig. 11, we compared I_0 (dashed line) and I_{eff} (solid line) for the case of $\Delta_{12} = -0.04$ meV. The results show that the significant steepness and high amplitude of the I_{eff} are associated with the ultrafast oscillations. Note that with the increase of $|\Delta_{12}|$ beyond 0.04 meV the steepness of I_{eff} reduces, reaching that of the applied field. With this, the coherent oscillations are damped. Note also that similar oscillations, although, with different phase were also seen in ρ_{22} (exciton population), suggesting coherently induced Rabi flopping (not shown) [2,3]. Combination of these results show that in QD-MNP systems the dynamics of exciton populations and plasmonic fields experienced by the QD are all coupled together.

In the case of positive detuning, as expected from the results shown in Fig. 8, the coherent dynamics of the QD-MNP systems behave quite differently. Here, as shown in Fig. 9(b), with increase of Δ_{12} no significant oscillation is generated. Instead, the rise time of P_{coh} undergoes further time delay. For $\Delta_{12} = 0.04$ meV (line 4), the system reaches a critical point wherein with a slight increase of Δ_{12} P_{coh}, the time delay becomes infinite and P_{coh} remains small at all time (line 5). This is the signature of transition from the B state, where P_{coh} is significant, to the D state. As we increase Δ_{12} beyond this, the coupling between the laser and the QD-MNP system reduces, and the coherent effects are diminished. Under this condition, the incoherent plasmonic field of the MNP starts to dominant (line 6).

The physics behind the results shown in Fig. 2 and the time delay seen in Fig. 9(b) can be explained considering the way Δ_{eff} and Λ_{eff} (coherently induced detuning and broadening of the QD) depend on the exciton population (or $\rho_{11} - \rho_{22}$) and the applied laser field intensity at the onset of the interaction of the QD-MNP system with the laser field. When I_0 is small (just before the laser rise time reaches the system) $\rho_{11} - \rho_{22}$ is large and Δ_{eff} and Λ_{eff} are significant. Therefore, the interaction between the QD and the laser field is suppressed and, as the rise time of the laser field reaches the system ρ_{22} cannot increase abruptly. As a result, Δ_{eff} and Λ_{eff} persist to be much larger than Δ_{12} and γ_{21}, respectively, even after the rise time of the applied field. When I_0 is large enough, ultimately the exciton density starts to ramp up, forcing $\Delta_{eff} \to \Delta_{12}$ and $\Lambda_{eff} \to \gamma_{21}$ (ρ_{11} and $\rho_{22} \to 0.5$). This allows the QD-MNP

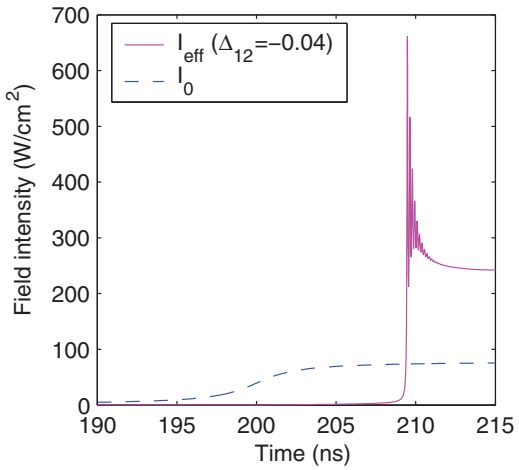

FIG. 11. (Color online) Applied field intensity (dashed line) and the effective field intensity experienced by the QD when $\Delta_{12} = -0.04$ meV. All other specifications are the same as those in Fig. 9.

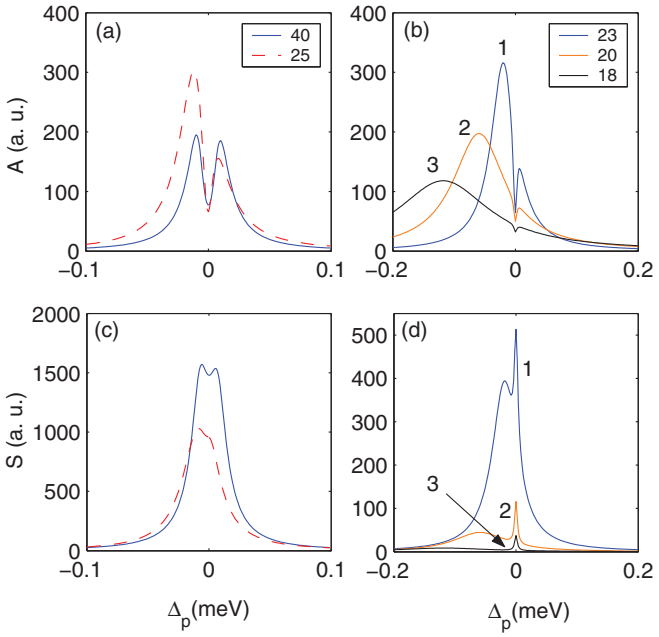

FIG. 12. (Color online) Variation of the absorption [(a) and (b)] and RF [(c) and (d)] of the QD for different R (legends in nm) when $I_0 = 0.5$ W/cm^2 and $\Delta_{12} = 0$. The numbers 1, 2, and 3 in Figs. 12(b) and 12(d) correspond to $R = 23$, 20, and 18 nm, respectively. All other specifications are the same as those in Fig. 2.

system to become more effectively engaged with the laser field, leading to the B state. For $I_0 < I_c$, however, the field is too weak to allow $\rho_{11} - \rho_{22} \to 0$. Therefore, the exciton population remains depressed at all times and the system is excited to the D state at all times. Note that the fact in the B state $\Delta_{\text{eff}} = \Delta_{12}$ and $\Lambda_{\text{eff}} = \gamma_{21}$ explains why in Fig. 3 we do not see broadening and red shifting, as one expects to see if a QD is close to an MNP.

The transition between the B and D states can be instantaneous when the laser intensity is high enough or R is sufficiently small. This can be clarified considering the fact that in the time domain this transition corresponds to the case when the time delay of the field experienced by the QD is increased from a finite value to infinity [Fig. 9(b)]. When the applied laser intensity is small or R is relatively large the B-D transition does not happen suddenly. This, in fact, is shown in Fig. 2 when $I_0 = 0.5$ W/cm^2. Under this condition we do not see any time delay in P_{coh}. Rather its value decreases with the reduction as depicted in Fig. 2 (triangles), independent of time. Under these conditions, one can study the intermediate state by either changing R considering I_0 is constant, or assuming R is fixed but vary I_0. The results shown is Fig. 12 show the evolution of absorption and RF of the QD-MNP considered in this paper when R is changed and $I_0 = 0.5$ W/cm^2, corresponding to the results shown in Fig. 2 (triangles). Note for $R = 40$ nm, the spectra contain two peaks, as one expects when a two-level system is coupled with a resonant laser. As R reduces, the longer wavelength absorption peak starts to red shift while it becomes stronger. For smaller R a sharp dip is formed, but no gain is generated [Fig. 12(b)]. In the case of RF, reduction of R generates a sharp peak at the laser wavelength.

VII. CONCLUSIONS

We studied quantum optical properties of QDs and dynamics of coherently normalized plasmonic fields of MNPs in QD-MNP systems driven by a laser field. The results showed that, depending on the collective states of such systems (bright and dark states), they could support very different optics. In the bright state, these systems exhibited standard optics, as those of isolated QDs, although the QDs and MNPs were very close to each other. Here the plasmonic effects only enhanced ac Stark shifts. We showed in this state the QD-MNP systems could support coherent oscillations of plasmonic fields. This led to strong enhancement of these fields via coherent dynamics of the systems over short periods of time. We showed that when the laser frequency became larger than that of the QD transition (position detuning) such coherent oscillations were smeared out. This suggested that the coherent exciton coupling can make the QD transition asymmetric. Under the steady-state condition, this can result in unique spectral features in the absorption of the QDs, including (i) enhancement of gain-absorption processes for negative detuning (bright state) and (ii) formation of a superfluorescent ultranarrow state that supports gain without inversion for positive detuning (dark state). We showed the reasons behind the ultrafast oscillations were not only the plasmonic field enhancement, but also the fact that coherent effects can make the variations of the effective field experienced by the QDs with time much faster than that of the applied field.

[1] M.-T. Cheng, S.-D. Liu, H.-J. Hao, and Q.-Q. Wang, Opt. Lett. **32**, 2125 (2007).
[2] S. M. Sadeghi, Nanotechnology **20**, 225401 (2009).
[3] S. M. Sadeghi, Phys. Rev. B **79**, 233309 (2009).
[4] Z. Lu and K.-D. Zhu, J. Phys. B **42**, 015502 (2009).
[5] R. D. Artuso and G. W. Bryant, Nano Lett. **8**, 2106 (2008).
[6] A. V. Malyshev and V. A. Malyshev, Phys. Rev. B **84**, 035314 (2011).
[7] J.-B. Li, N.-C. Kim, M.-T. Cheng, L. Zhou, Z.-H. Hao, and Q.-Q. Wang, Opt. Express **20**, 1856 (2012).
[8] J.-Y. Yan, W. Zhang, S. Duan, X.-G. Zhao, and A. O. Govorov, Phys. Rev. B **77**, 165301 (2008).
[9] R. D. Artuso and G. W. Bryant, Phys. Rev. B **82**, 195419 (2010).
[10] S. M. Sadeghi, L. Deng, X. Li, and W.-P. Huang, Nanotechnology **20**, 365401 (2009).
[11] W. Zhang and A. O. Govorov, Phys. Rev. B **84**, 081405 (2011).
[12] A. Hatef, S. M. Sadeghi, and M. R. Singh, Nanotechnology **23**, 065701 (2012).
[13] Y. He and K.-D. Zhu, Nano. Res. Lett. **7**, 95 (2012).
[14] S. G. Kosionis, A. F. Terzis, S. M. Sadeghi, and E. Paspalakis, J. Phys.: Condens. Matter **25**, 045304 (2013).
[15] S. Evangelou, V. Yannopapas, and E. Paspalakis, Phys. Rev. A **86**, 053811 (2012).
[16] S. M. Sadeghi and R. G. West, J. Phys.: Condens. Matter **23**, 425302 (2011).
[17] S. M. Sadeghi, J. Nanopart. Res. **14**, 1184 (2012).
[18] B. R. Mollow, Phys. Rev. A **5**, 2217 (1972).
[19] X. Xu, B. Sun, P. R. Berman, D. G. Steel, A. S. Bracker, D. Gammon, and L. J. Sham, Science **317**, 929 (2007).
[20] W. Zhang, A. O. Govorov, and G. W. Bryant, Phys. Rev. Lett. **97**, 146804 (2006).
[21] K. L. Kelly, E. Coronado, L. L. Zhao, and G. C. Schatz, J. Phys. Chem. B **107**, 668 (2003).
[22] E. Cottancin, G. Celep, J. Lerme, M. P. J. R. Huntzinger, J. L. Vialle, and M. Broyer, Theor. Chem. Acc. **116**, 514 (2006).
[23] A. S. Manka, H. M. Doss, L. M. Narducci, P. Ru, and G.-L. Oppo, Phys. Rev. A **43**, 3748 (1991).
[24] S. M. Sadeghi, Nanotechnology **21**, 455401 (2010).
[25] G. Grynberg and C. Cohen-Tannoudj, Opt. Commun. **96**, 150 (1993).
[26] M. O. Scully and M. S. Zubairy, *Quantum Optics* (Cambridge University Press, Cambridge, 1997).